Electronic Supplementary Material (ESI) for RSC Advances.


**Supplementary Information**

# Double-Exponential Refractive Index Sensitivity of Metal-Semiconductor Core-shell Nanoparticle: The Effects of Dual-Plasmon Resonances and Red-shift

**Hailong Zhang[1],Pengfei Cao*[1, 2], Jie Dou[1], Lin Cheng[1], Tiaoming Niu[1], Guanmao Zhang[1]**

[1]School of Information Science and Engineering, Lanzhou University, Lanzhou 730000, China

[2]Kirchhoff-Institute for Physics, Im Neuenheimer Feld 227, 69120 Heidelberg, Germany

The extinction spectra of Au@$Cu_{2-x}S$ core-shell nanoshells (CSNs) in a variety of shell thicknesses and core radii are shown in Figure s1. With a $Cu_{2-x}S$ shell thickness variation of between 2 nm and 10 nm (Figure s1a), the $\omega+$ mode shows a blue-shift trend between 518 nm and 504 nm (see Tabure s1). However, with the Au core variation between 10 nm and 30 nm (Figure s1b), the $\omega+$ mode shows a slight red-shift tendency between 501 nm and 511 nm (see Tabure s2). Herein, according to the equation 6 in the paper, the increase of the shell thickness could lead to an enlargement of the $\omega+$, therefore, the $\omega+$ shows a slight blue-shift tendency.

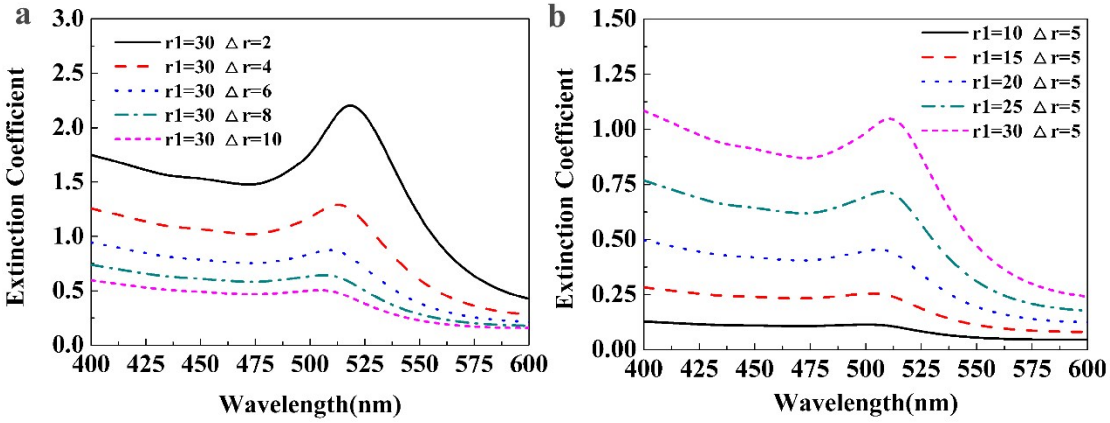


**Figure s1:** Extinction spectra of Au@$Cu_{2-x}S$ CSNs at different shell thicknesses and core radius. a) Extinction spectra of Au@$Cu_{2-x}S$ CSNs at different shell thicknesses with a constant core radius of 30 nm; b) Extinction spectra of Au@$Cu_{2-x}S$ CSNs at different core radii with a constant shell thickness of 5 nm.

**Table s1:** The wavelength of $\omega+$ mode.

| $r_1/r_2$(nm) | 30/32 | 30/34 | 30/36 | 30/38 | 30/40 |
|---|---|---|---|---|---|
| Wavelength(nm) | 518 | 513 | 509 | 507 | 504 |

**Table s2:** The wavelength of $\omega+$ mode.

| $r_1/r_2$(nm) | 10/15 | 15/20 | 20/25 | 25/30 | 30/35 |
|---|---|---|---|---|---|
| Wavelength(nm) | 501 | 503 | 506 | 508 | 511 |

The extinction spectra of the Au@$Cu_{2-x}S$ CSNs are investigated (Figure s2). We see that the localized surface plasmon resonance (LSPR) peak of $\omega+$ mode shows a red-shift tendency, but it is relatively weak with the changes of the surrounding medium. It demonstrates that the increase of polarizability of the dielectric media has almost no effect on LSPR forming of the conduction electrons oscillating on the inner surface of the $Cu_{2-x}S$ shell under $\omega+$ mode.

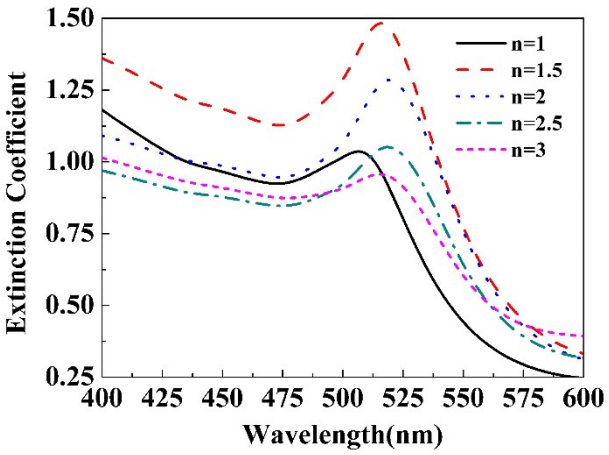


**Figure s2:** Extinction spectra of Au@$Cu_{2-x}S$ CSNs in different refractive indexes with $r_1$ = 35 nm and $r_2$ = 40 nm.

The Extinction spectra of Au@$Cu_{2-x}S$ CSNs in different refractive indexes of the surrounding media are calculated (Figure s3, s4). By calculating the difference in value between the resonance wavelength in $n > 1.0$ and the resonance wavelength in $n = 1.0$, we obtained the LSPR shift in different refractive indexes of the surrounding

media (Figure 4). Here, we show how the extinction spectrum of the Au@$Cu_{2-x}S$ CSNs change as the thickness of the $Cu_{2-x}S$ shell is increased but with a constant core radius of 30 nm (Figure s3). We also show how the core radius of Au is increased but with a constant shell thickness of 5 nm (Figure s4). When the refractive index n is 3.0 (Figure s3), the LSPR shift of the Au@$Cu_{2-x}S$ CSNs corresponding to the $\omega$- mode is 474 nm (from 1315 nm to 1789 nm) with the change of the shell thickness when the refractive index is 3.0. However, the LSPR shift of the Au@$Cu_{2-x}S$ CSNs is only 161 nm (from 1849 to 1688 nm) under the same refractive index (Figure s4) with the change in core radius. The resonance wavelength shift with a change in shell thickness is larger than that with the variation in core radius, which is more evident at large refractive indexes media.

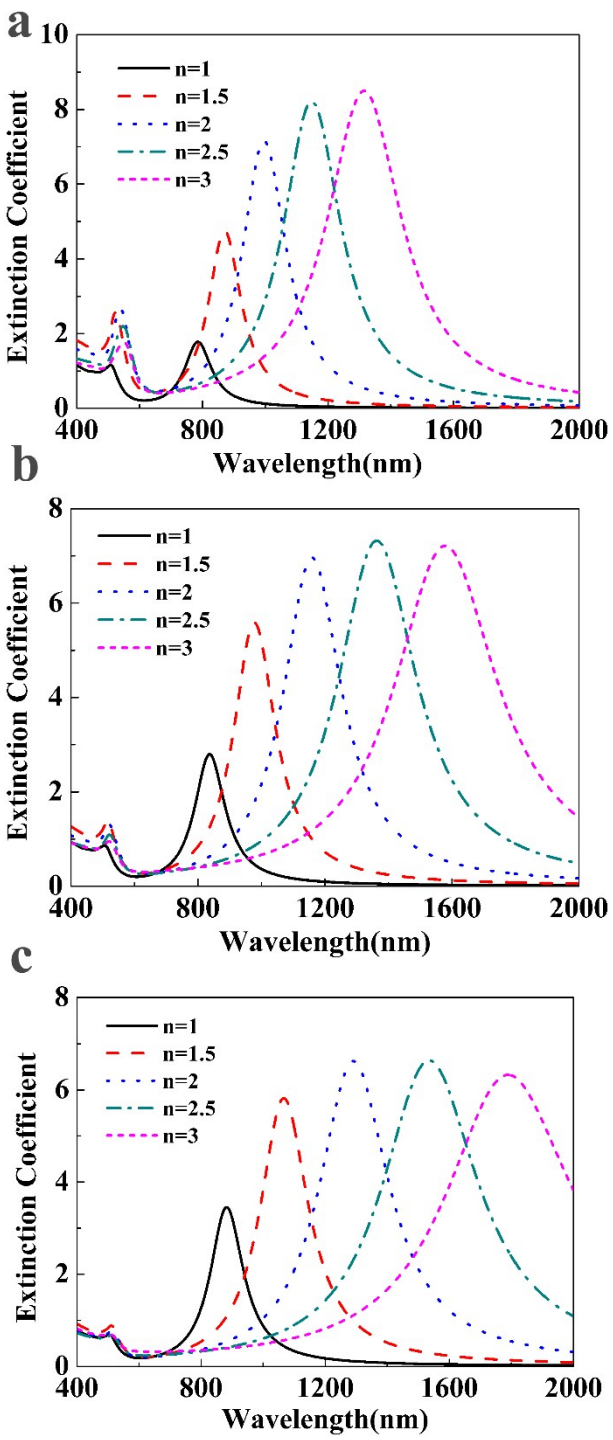


**Figure s3:** Extinction spectra of Au@$Cu_{2-x}S$ CSNs at different shell thickness but with a constant core radius of 30 nm. a) Extinction spectra of Au@$Cu_{2-x}S$ CSNs with the shell thickness of 2 nm; b) Extinction spectra of Au@$Cu_{2-x}S$ CSNs with the shell thickness of 4 nm; c) Extinction spectra of Au@$Cu_{2-x}S$

CSNs with the shell thickness of 6nm.

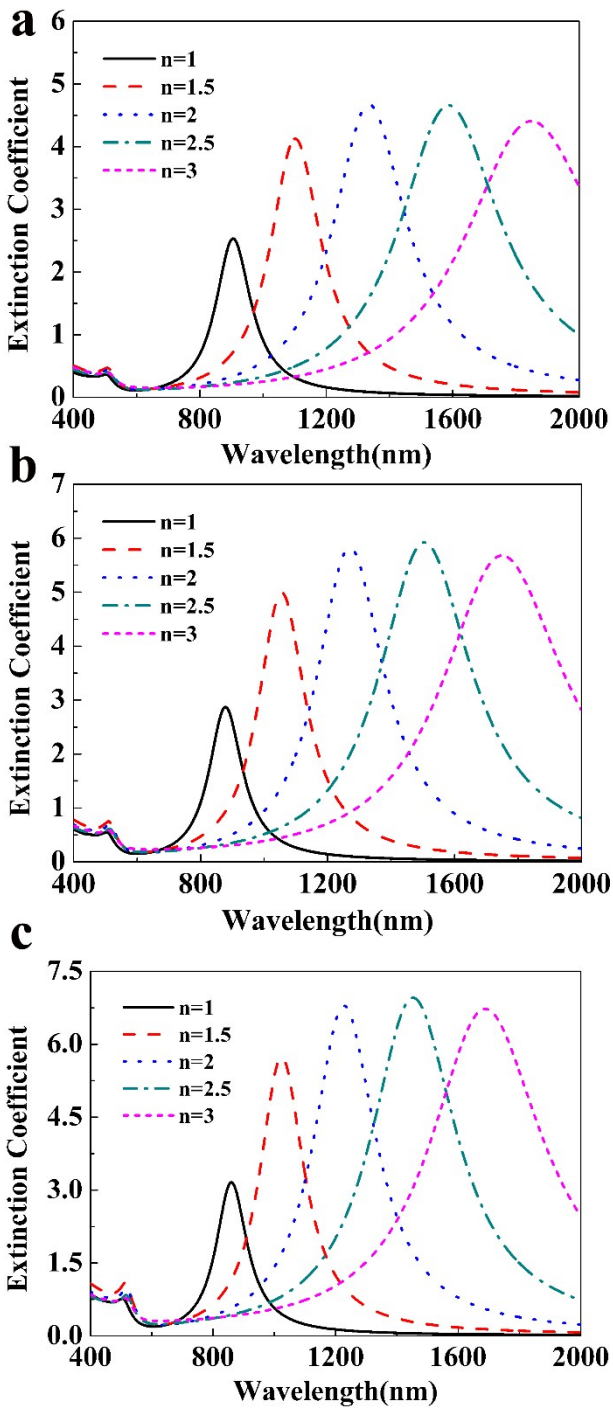


**Figure s4:** Extinction spectra of Au@$Cu_{2-x}S$ CSNs at different core radius but with a constant shell thickness of 5 nm. a) Extinction spectra of Au@$Cu_{2-x}S$ CSNs with the core radius of 20 nm, b) Extinction spectra of Au@$Cu_{2-x}S$ CSNs with the core radius of 25 nm, c) Extinction spectra of Au@$Cu_{2-x}S$ CSNs with

the core radius of 30nm.

Here, we determine the sensitivities of the resonance wavelength to the surrounding medium refractive indexes by calculating the spectra of the Au@Ag CSNs with two surrounding media, with refractive indices $n$ equal to 0.5 and 1.0, which are different from the Au@$Cu_{2-x}S$ CSNs. We do this because the only resonance wavelength of Au@Ag CSNs reflects the $\omega+$ mode, instead of $\omega-$ mode, when the refractive indices are larger than 1.0 (Figure s5). The sensitivity of the Au@Ag CSNs rises double-exponentially with the enlarging of the shell-thickness to core-radius ratio (Figure s6), which is like that of the Au@$Cu_{2-x}S$ CSNs. Meanwhile, the local electric field pattern and electric charge distribution are also calculated (Figure s7). The same types of charges are concentrated on both inner and outer Au surfaces along the incident polarization; so the strong local field appears at both the inner and outer surfaces of the Ag shell, which are like those of the Au@$Cu_{2-x}S$ CSNs.

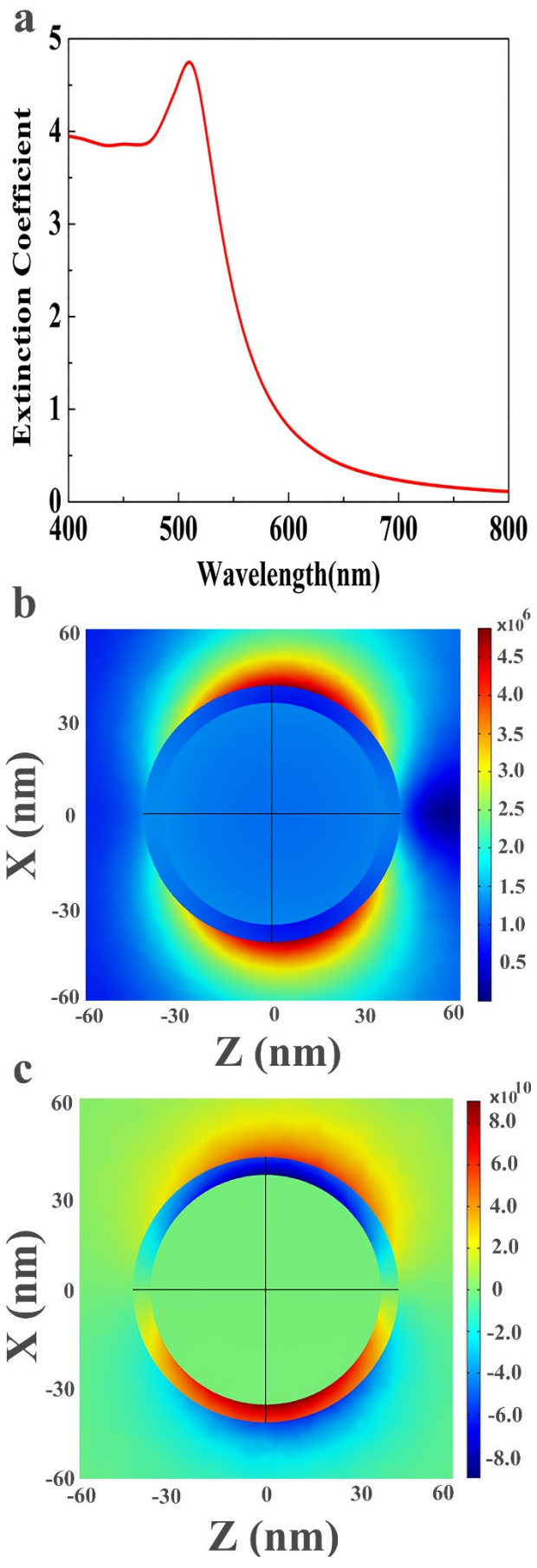
a
Extinction Coefficient
0
1
2
3
4
5
400
500
600
700
800
Wavelength(nm)
b
X (nm)
Z (nm)
60
30
0
-30
-60
x10^6
4.5
4.0
3.5
3.0
2.5
2.0
1.5
1.0
0.5
c
X (nm)
Z (nm)
x10^10
8.0
6.0
4.0
2.0
0
-2.0
-4.0
-6.0
-8.0

**Figure s5:** Extinction spectra and local electric field pattern of Au@Ag CSNs in a refractive index of 1.2. a) Extinction spectra of Au@Ag CSNs; b) Electric field of the Au@Ag CSNs; c) Charge distribution of the Au@Ag CSNs.

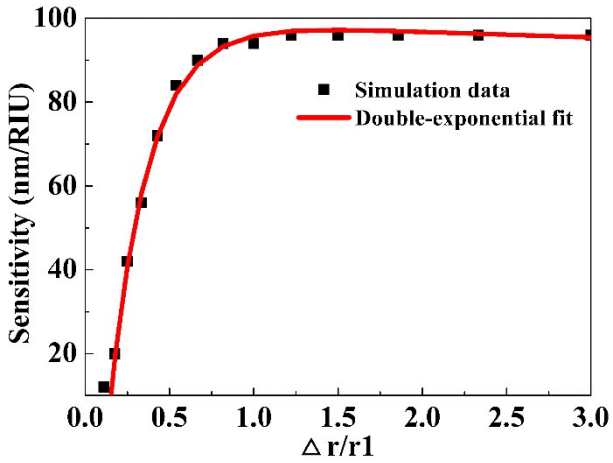


**Figure s6:** The sensitivity of Au@Ag CSNs falls double-exponentially with the increasing $\Delta r/r_1$ as seen from the fit (red line) to the double-exponential decay with $a$ = 99.53±10.89, $b$ = –0.01406±0.05158, $c$ = 170.4±34.1, and $d$ = 4.289±1.301.

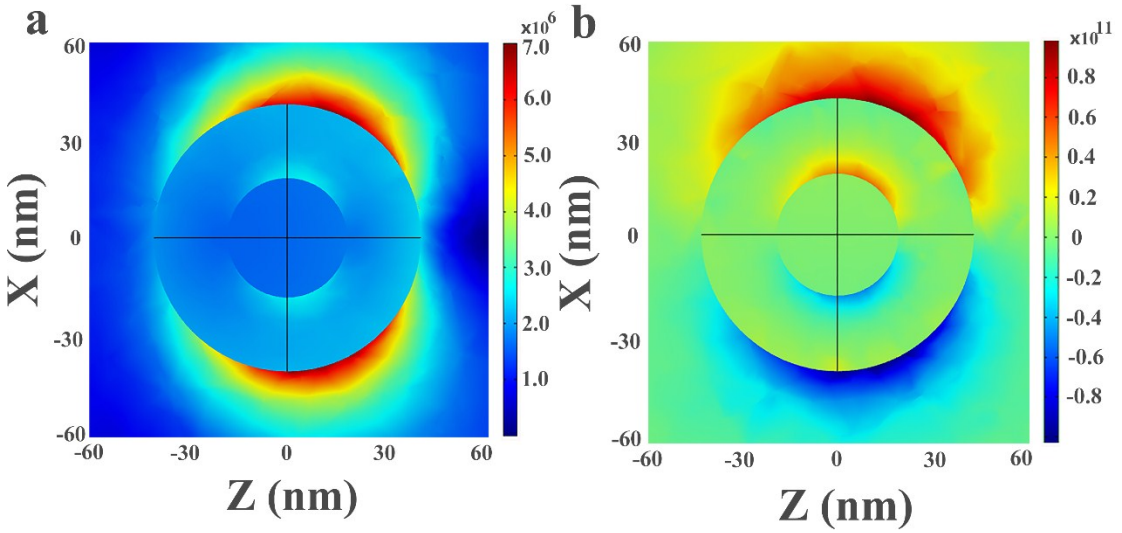


**Figure s7:** Local electric field and charge pattern of Au@Ag CSNs with $r_1$ =20 nm and $r_2$ =40 nm, while the resonance wavelength is 377 nm a) Local electric

field; b) Electric charge distribution .

However, although the sensitivities of the Au@Ag and Au@$Cu_{2-x}S$ CSNs rise with the increase of the ratio of shell-thickness to core-radius, the sensitivity of Au@Ag is far smaller than that of the Au@$Cu_{2-x}S$ CSNs. To find out why this is different, we calculated the positive imaginary portion of the dielectric constant comparison of the Au@Ag and Au@$Cu_{2-x}S$ CSNs (Figure s8). Here, the positive imaginary portion of the Au@$Cu_{2-x}S$ CSNs is smaller than that of the Au@Ag, leading to the stronger LSPR[1] and higher sensitivity[2]. Furthermore, when the surrounding refractive index is small[3], the polarizability from the surrounding media is weak, which results in the lower sensitivity.

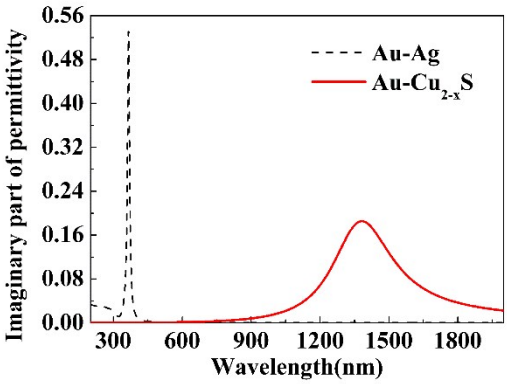


**Figure s8:** The positive imaginary portion of dielectric constant comparison of the Au@Ag and Au@$Cu_{2-x}S$ CSNs.

# References:


1.Laura B. Sagle, Laura K. Ruvuna, Julia A. Ruemmele, Richard P. Van Duyne. *Nanomedicine*, 2011,6,1447.

2.Jagmeet Singh Sekhon, S. S Verma. *Plasmonics*, 2011,6,311.

3.Jian Zhu, Xing-chun Deng. *Sensors and Actuators B: Chemical*, 2011,155,843.